Estimating the ashfall distribution for a small eruption using ellipse-approximated isopach analysis: How many seeking points are required to determine a suitable axis?

Yasuhisa Tajima (yasu-tajima@pd6.so-net.ne.jp)
Nippon Koei Co., Ltd.

Express Letter

Keywords: Kirishima Volcano Group, Shinmoedake, Ashfall, Volume, Small eruption

Posted Date: April 7th, 2021

DOI: https://doi.org/10.21203/rs.3.rs-376659/v1

Version of Record: A version of this preprint was published at Earth, Planets and Space on July 30th, 2021. See the published version at https://doi.org/10.1186/s40623-021-01483-4.

Abstract

A volcanic ash eruption began on March 3, 2018, and a lava flow was observed on March 6 at Shinmoedake volcano in the Kirishima Volcano Group. The small ash eruptions continued until June 27, 2018. The amounts of volcanic ashfall around Shinmoedake volcano from these eruptions were observed, and the volcanic ashfall volumes for each eruption were analyzed. However, many cases of small eruptions were insufficient observation points to determine the ashfall volumes. Therefore, the ellipse-approximated isopach (EAI) method was used. However, the EAI method requires verification seeking points to determine the angle of the calculation axis including two calculation points to perform the analysis. In this study, the ashfall amount values at some locations from one eruption on June 27, 2018 were observed, and the EAI analysis was conducted to determine the ashfall distribution using one to four seeking points. It is considered that a suitable axis requires three seeking points to determine the EAI distribution.

Introduction

Shinmoedake volcano in the Kirishima Volcano Group (Fig. 1) has undergone repeated magmatic eruptions and quiet periods lasting hundreds to thousands of years and is currently in an active magmatic eruption period (Tajima et al., 2013a). Subplinian eruptions were produced from 1716–1717 and in 2011 (Imura and Kobayashi, 1991; Nakada et al., 2013). The recent activities were small ash-producing eruptions from October 11–17, 2017. And lava eruptions occurred in 2018 with similar small eruptions from March 1–6, 2018 before the lava producing and Vulcanian or small eruptions until June 27 after the lava producing. Small amounts of volcanic ash were emitted before the 2011 Subplinian eruptions and the 2018 lava eruptions. Therefore, rapid and accurate determination of the volumes of volcanic ash produced by small eruptions before a peak magmatic eruption is an important framework for future monitoring. Additionally, the sequence of frequent Vulcanian or small eruptions after a peak magmatic eruption is indispensable for predicting the end of activity.

Several methods for estimating the volume of tephra using isopleths have been proposed. The tephra volume is estimated using isopleths in an integrating plot of log (T) against log (A) with the distribution area (A) and thickness (T) of the deposit (Rose et al., 1973). Furthermore, an exponentially decreasing plot of log (T) against log ($\sqrt{A}$) is used for larger tephra (Pyle, 1989). Two proximal and distal exponential rates (κ) of the plot of log (T) against log ($\sqrt{A}$), which change at the break in the slope, have been used to calculate the volume (Fierstein and Nathenson, 1992). A power method using a plot of log (T) against log ($\sqrt{A}$) was used to estimate the volume of the tephra (Bonadonna and Houghton, 2005). The volume/mass of the ashfall can be calculated by segment integration, which introduces segments to a thickness/weight-area plot (Takarada et al., 2001, 2002, 2016). The Weibull distribution has recently been proposed as a method for estimating tephra volume (Bonadonna and Costa, 2012, 2013). However, many isopleths are required to accurately estimate the tephra or ashfall volume over large areas when using such methods. Meanwhile, obtaining the volume from a single isopleth has also been proposed (Hayakawa, 1985). The equation is $V = 12.2TA$, which is approximately based on the tephra volumes

obtained by Walker (1980, 1981). Additionally, the following fixed equation has been proposed for the minimum volume obtained using some tephra isopleths as V = 3.69TA (Legros, 2000).

Tajima et al. (2013b) combined the concepts of the decay rate of the thickness of the ashfall layer with an increasing area approximated as a power of −1 (Aramaki and Hayakawa, 1982) and ash distribution approximated as an ellipse (Pyle, 1989; Bursik et al., 1992; Sulpizio, 2005). They argued that the mass of a volcanic ash deposit could be estimated with two observation points and an accurate distribution (calculation) axis by assuming an ellipse similar to the ellipse-approximated isopach (EAI) method. Additionally, ashfall verification values called "seeking points" have been adopted to determine the calculation axis in the EAI method. However, discussions on the required number of seeking points are limited. In this study, the amounts of ashfall from the June 27, 2018 eruption were observed to determine the number of points required to accurately estimate the calculation axis. Changing the number of seeking points produced variable ashfall distributions and the resulting variations indicated an appropriate number of seeking points.

June 27 eruption and sample collection

A small eruption occurred at Shinmoedake volcano at 15:34 Japan Standard Time (JST) on June 27, 2018. The column color was gray-white with a height of 2200 m, according to records from the Japan Meteorological Agency (JMA: KLMO-JMA, RVOWC-FRH-JMA, 2018). The eruption column passed over the office in the town of Takaharu, according to the live camera image captured by UMK TV Miyazaki, and volcanic ash fell in central Takaharu east-northeast of Shinmoedake (Fig. 2A).

The ashfall distribution of the June 27 eruption was surveyed between June 28 and June 29, and volcanic ash was sampled as follows. Areas with minimal wind-sweeping were selected, because wind sometimes removes volcanic ash. For volcanic ash collection, sampling areas, such as park benches, facility concretes, public dust boxes, mail posts, and the outdoor units of air conditioners, were not in contact with the ground. A folding ruler was used to measure a square sampling area, and volcanic ash was placed into a sample bag using a dustpan and a brush. Volcanic ash at a monitoring point installed in the ashfall area was sampled in a small, clear plastic cup (Table S1 of the Supplemental Material). Furthermore, the amount of volcanic ash was recorded under the following categories: abundant (++), normal (+), faint (−), and not detected (nd) when not sampled (e.g., on leaves). A Garmin handheld GPS or a digital camera equipped with a GPS function was used to measure the latitude and longitude at the observation points. The weights of the dried samples were measured and converted into the ashfall amount (g/m^2) of the collection area.

In the field survey, the amounts of ashfall exceeded 60 g/m^2 at Hinamoridai and Suigenchi (Fig. 2A). The southern limit of the ashfall distribution was in Kozuka, near the Takasaki River and the northern limit was in Aikubo. The gray break lines indicate the ashfall distribution limits and the isopleth of 40 g/m^2. Accretionary lapilli were approximately 1 mm in diameter at the Suigenchi (61.2 g/m^2) point. No rainfall was registered in central Takaharu during the ashfall, but weak rainfall in Hinamoridai reported in the

interview might have fallen in the mountainous area. Ash particles were divided five types as black glass with sometimes drop-like shapes (14%), gray glass fragments with fresh and sharp shapes (56%), red fragments with sharp shapes (13%), Plagioclase (11%), and Pyroxenes (5%) (Fig. 2B). In addition, microscopic observations revealed that some red fragments had secondary minerals and rounded shapes. Ash particles were smaller than 2 mm in diameter in the observed area (Fig. 2C). This was not significantly different from those of the 2011 Vulcanian or small eruptions (Suzuki et al., 2013).

Methods

EAI analysis method

The EAI analysis is a volume (mass) estimation tool for an ashfall deposit that sets four conditions, including the fixed crater/vent location (P_0), observation point 1 (P_1), observation point 2 (P_2), and the calculation axis (Fig. 3; Tajima et al., 2013b). The vent location of this eruption was set at 31.911598° N, 130.882959° E based on the 2018 lava production center observed by the Geospatial Information Authority of Japan (GSI) (2018) on April 1, 2018. This value was converted into a point on a rectangular coordinate system using the GSI website (Kawase, 2011; Geospatial Information Authority of Japan, 2013). The latitudes and longitudes of the observation points were also converted into rectangular coordinate system values, which were plotted on a coordinate system as an abscissa (x) of east positive and an ordinate (y) of north positive from an origin P_0 (0, 0) representing the vent location. A preliminary calculation axis was set based on the entire distribution and added observation points to the map. Two observation points with a preliminary axis introduced similar ellipses. Ellipses 1 and 2 were assigned to observation points P_1 (x_1, y_1) and P_2 (x_2, y_2), respectively. The locations of P_0, P_1, and P_2 on ellipse 1 were calculated as follows, where T_1 and T_2 are the thicknesses of P_1 and P_2, respectively:

$$P_0 = (0,0),\ P_1 = (x_1, y_1),\ P_2{}' = \left(\sqrt{\frac{T_2}{T_1}} x_2,\ \sqrt{\frac{T_2}{T_1}} y_2 \right). \quad (1)$$

The major calculation (a_1) and minor orthogonal (b_1) axes lengths of ellipse 1 can be calculated as follows:

$$a_1 = \frac{x_1^2 y_2^2 - x_2^2 y_1^2}{2\left(x_1 y_2^2 - \sqrt{\frac{T_2}{T_1}} x_2 y_1^2\right)},\ b_1 = \sqrt{\frac{a_1^2 y_1^2}{2a_1 x_1 - x_1^2}}. \quad (2)$$

The ashfall volume was calculated as an area (A) and volume (V) using the following equation from Hayakawa (1985) and Legros (2000):

$$A = \alpha T^{-1}. \quad (3)$$

The volume integral is:

$$V = \int_m^n \alpha A^{-1} dT \quad (4)$$

In Tajima et al. (2013b), m is 10,000 m^2 (according to Takarada et al., 2001); and n is the area surrounded by the isopleth of 0.1 g/m^2, according to observations at Sakurajima volcano. The amount of ashfall (g/m^2) was converted into a thickness of 1 g/cm^3 based on the apparent density of ashfall deposits from the small eruption of Shinmoedake volcano on January 19, 2011 (Tajima, 2014).

The goal of this study is to determine the number of seeking points required to obtain an accurate calculation axis. Thus, we examined the following. First, calculation points of 67.3, 61.2, 93.8, and 43.7 g/m^2 were selected that were less affected by weather and sampling error (Fig. 2A). The values contained in parentheses in Fig. 2A were only used as supporting values, as they might have been affected by the bending column or wind. Cases of one, two, three, or four seeking points were examined for verification. The following seeking points were used the observation point results at 67.3, 61.2, 26.9, 43.7, 93.8, and 0.8 g/m^2. The analysis of the number of seeking points cases calculated 24, 36, 24, and 6 combinations were obtained with one, two, three, and four seeking points excluded two calculation points, respectively. The observed and calculated values did not match, because EAI analysis uses geometry. Therefore, an optimal solution (determined axis) was defined as the minimum value of the sum of $(Obs./Cal.-1)^2$ by the amounts of ashfall for an axis of 0.1°. The ashfall distribution derived by the EAI method was defined as the EAI distribution, and the volume (mass) was called the EAI ashfall volume (m^3), or mass (t).

Results

The EAI distributions were calculated by the EAI analysis for one to four seeking points. And the angle of the determined axis, ellipse aspect ratio (half radius of the orthogonal/calculation axes), and the EAI volume were obtained for every calculation result (Tables S2, S3, S4, and S5). The EAI volumes were reported with three significant figures. The angle of the calculation axis ranged from 0° to 360° clockwise, starting from the east. Maximum, average, and minimum examples of the EAI distributions of each seeking point case were obtained (Fig. 4). And the limit of the EAI distribution (indicated by the gray dashed line in Fig. 3) was 0.1 g/m^2, based on Tajima et al. (2013b). The mean value and standard deviation of the EAI volume were estimated for each seeking point case using the probability density distribution (Fig. 5).

For the 24 one-point seeking calculations, the average axis angle was 345.9°, and the maximum-minimum angle difference was 2.8°. The average ellipse aspect ratio was 0.042 and ranged from 0.026 to 0.057. The average EAI volume was 2.96×10^3 m^3 and ranged from and 0.68×10^3 to 4.74×10^3 m^3. The standard deviation of the EAI volume was 0.93×10^3 m^3, based on the one-point seeking calculations (Fig. 5). The EAI distribution limit was narrower than the observed distribution limit of the minimum result, which was consistent with the smaller ellipse aspect ratio. The EAI and observation distribution limits

were similar to the average result. However, the EAI distribution limit was wider than the observed distribution limit of the maximum result (Fig. 4A).

For the 36 two-point seeking calculations, the average axis angle was 345.9°, and the maximum-minimum angle difference was 1.6°. The average ellipse aspect ratio was 0.043 and ranged from 0.034 to 0.056. The average EAI volume was 2.76×10^3 m^3 and ranged from 1.62×10^3 to 4.44×10^3 m^3. The standard deviation of the EAI volume was 0.49×10^3 m^3 (Fig. 5). The distribution limit of the minimum result was almost consistent with the observation result, but the 40 g/m^2 isopleth axis of the EAI distribution was shorter. The EAI distribution limit of the average result was consistent with the observation. The EAI distribution limit of the maximum result was wider than that of the observation result (Fig. 4B).

For the 24 three-point seeking calculations, the average axis angle was 345.8°, and the maximum-minimum angle difference was 0.7°. The average ellipse aspect ratio was 0.043 and ranged from 0.035 to 0.054. The average EAI volume was 2.66×10^3 m^3 and ranged from 2.09×10^3 to 3.28×10^3 m^3. The standard deviation of the EAI volume obtained from the three-point seeking calculations was 0.30×10^3 m^3 (Fig. 5). The EAI distribution limits of the minimum, mean, and maximum volumes in this case were very similar to the observation results. However, the volumes differed depending on the length of the major axis (Fig. 4C).

For the six four-point seeking calculations, the average axis angle was 345.9°, and maximum-minimum angle difference was 0.4°. The average ellipse aspect ratio was 0.043 and ranged from 0.035 to 0.052. The average EAI volume was 2.63×10^3 m^3 and ranged from 2.22×10^3 to 2.98×10^3 m^3. The standard deviation of the EAI volume obtained from the four-point seeking calculations was 0.28×10^3 m^3 (Fig. 5). The EAI distribution limits of the minimum, mean, and maximum volumes in this case were very similar to the observation result (Fig. 4D).

Discussion And Conclusion

The distribution limit of the EAI analysis of the minimum value of the residual sum of the squares of the seeking with three and four points and the limit of the field observation almost correspond with the geometric calculation. The relationship between the area and thickness of the larger tephra is generally expressed as the square root of the isopleth area (e.g., Pyle 1989; Sparks et al., 1992; Fierstein and Nathenson, 1992). However, the plot of the thickness versus the square root of the isopleth area of the tephra contain break-in-slopes depending on the differences in the Reynolds number based on the grain size, density, and eruption height (Rose, 1993; Bonadonna et al., 1998). Intermediate- and low-Reynolds-number particles in the distal area are better described by the power-law behavior. This tendency is significant in the lower columns (Bonadonna et al., 1998). The ashfall of small Vulcanian eruptions can be approximated by the power-law function, because ashfall is composed of grains smaller than 2 mm (78 wt. % in 2 and 3 φ in Fig. 2C) deposited at a column height of less than 10 km. The ashfall distribution of small eruptions from Sakurajima and other volcanoes exhibited approximately straight

lines in the thickness versus isopleth area, suggesting power behavior (Tajima et al., 2013b; Oishi et al., 2018). The EAI method approximated with a power of −1 may be well-distributed under Vulcanian or small magmatic ashfall conditions. Additionally, the creation of accretionary lapilli did not significantly impact power law behavior in this case.

The standard deviations of the EAI volume decreased, and the average values slightly decreased when the number of seeking points increased from one to four (Fig. 5). The standard deviations and mean values of the seeking cases with three and four points were very similar. Therefore, at least three seeking points are desirable. And at least two are required when estimating the axis using only the seeking points. The EAI volume from the three-point seeking cases in this study was $2.66 \pm 0.60 \times 10^3$ m^3 (2σ). The volumes calculated by V = 12.2TA (Hayakawa, 1985) and V = 3.69TA (Legros, 2000) were 3.0×10^3 and 0.9×10^3 m^3 based on the 40 g/m^2 isopleth, respectively. The average EAI volume of the three-point seeking case between these two volumes is acceptable. In another study, the EAI volume was between the exponential decay value (Fierstein and Nathenson, 1992) and area-thickness product calculation value at V = 12.2TA (Tajima, 2014). Therefore, the volume calculated by the EAI method is acceptable when compared to that of those methods. Thus, the EAI distribution (axis) determined using the minimum value of the residual sum of the squares could represent the observation results in the proximal area of the Vulcanian or small ashfall eruptions.

This study suggests that ashfall distribution could be mechanically estimated within a certain accuracy by the EAI analysis, where at least five well observation values are taken. However, we know the tephra distribution is not always symmetrical across the axis and that the distribution axis may be biased. The eruption column may spread in a concentric circular shape around the crater with very weak wind. In these cases, ashfall distribution analysis by the EAI is possible, but the accuracy of the EAI volume may decrease. In small eruptions of the Sakurajima volcano, the high- and low- level wind directions are different. Therefore, even one eruption may produce ashfall in different directions (Poulidis et al., 2017, 2019). The selection of observation locations and analysis techniques must be improved in such conditions. This research has the potential to be applied to eruption analysis and to tephra fields.

List Of Abbreviations

EAI: Ellipse-approximated isopach

JST: Japan Standard Time

JMA: Japan Meteorological Agency

KLMO-JMA: Kagoshima Local Meteorological Office, JMA

RVOWC-FRH-JMA: Regional Volcanic Observation and Warning Center, Fukuoka Regional Headquarters, JMA

GSI: Geospatial Information Authority of Japan

Declarations

Availability of data and materials

The data of the vent location used the website data of the GSI (https://www.gsi.go.jp/BOUSAI/h30kirishima-index.htm).

Competing interests

Not applicable.

Funding

Not applicable.

Author Contribution

YT designed the research, performed data processing, analysis, discussions and interpretation of the results, and wrote this paper.

Acknowledgments

The author thanks member of Hinamori Auto Camp for helping with the ashfall information and Y. Shinozuka and A. Hasegawa of Nippon Koei for helping in the laboratory. This study was edited for English by Editage (www.editage.com).

References

Aramaki S, and Hayakawa Y (1982) Ash fall during the April 26, 1982 eruption of Asama volcano. Bull Volcanol Soc Japan 27: 203–215 (in Japanese). doi.org/10.18940/kazanc.27.3_203.

Bonadonna C, Costa A (2012) Estimating the volume of tephra deposits: A new simple strategy. Geology 40: 415-418. doi.org/10.1130/G32769.1.

Bonadonna C, Costa A (2013) Plume height, volume, and classification of explosive volcanic eruptions based on the Weibull function. Bull Volcanol 75: 742. doi.org/10.1007/s00445-013-0742-1.

Bonadonna C, Houghton BF (2005) Total grain-size distribution and volume of tephra-fall deposits. Bull Volcanol 67: 441-456. doi.org/10.1007/s00445-004-0386-2.

Bonadonna C, Ernst GGJ, Sparks RSJ (1998) Thickness variations and volume estimates of tephra fall deposits: the importance of particle Reynolds number. J Volcanol Geotherm Res 81: 173–187. doi.org/10.1016/S0377-0273(98)00007-9.

Bursik MI, Sparks RSJ, Gilbert JS, Carey SN (1992) Sedimentation of tephra by volcanic plumes: I. Theory and its comparison with a study of the Fogo A plinian deposit, Sao Miguel (Azores). Bull Volcanol 54: 329–344. doi.org/10.1007/BF00301486.

Fierstein J, Nathenson M (1992) Another look at the calculation of fallout tephra volumes. Bull Volcanol 54: 156–167. doi.org/10.1007/BF00278005.

Geospatial Information Authority of Japan (2013) https://vldb.gsi.go.jp/sokuchi/surveycalc/surveycalc/bl2xyf.html. Accessed 1 March 2021.

Geospatial Information Authority of Japan (2018) https://www.gsi.go.jp/BOUSAI/h30kirishima-index.htm. Accessed 1 March 2021.

Hayakawa Y (1985) Pyroclastic geology of Towada volcano. Bull Earthq Res Inst Univ Tokyo 60: 507–592.

Imura R, Kobayashi T (1991) Eruptions of Shinmoedake Volcano, Kirishima Volcano Group, in the Last 300 Years. Bull Volcanol Soc Japan 36: 135-148 (in Japanese). doi.org/10.18940/kazan.36.2_135.

KLMO-JMA, RVOWC-FRH-JMA (2018) Volcanic Activity of Kirishimayama Volcano （September 1, 2017–September 30, 2018）. Report of Coordinating Committee for Prediction of Volcanic Eruption 131: 280–350 (in Japanese).

Kawase K (2011) A More Concise Method of Calculation for the Coordinate Conversion between Geographic and Plane Rectangular Coordinates on the Gauss-Krüger Projection. GSI journal 121: 109–124 (in Japanese).

Legros F (2000) Minimum volume of tephra fallout deposit estimated from a single isopach. J Volcanol Geotherm Res 96: 25–32. doi.org/10.1016/S0377-0273(99)00135-3.

Nakada S, Nagai M, Kaneko T, Suzuki Y, Maeno F (2013) The outline of the 2011 eruption at Shinmoe-dake (Kirishima), Japan. Earth Planet Space 65: 475–488. doi.org/10.5047/eps.2013.03.016.

Oishi M, Nishiki K, Geshi N, Furukawa R, Ishizuka Y, Oikawa T, Yamamoto T, Nanayama F, Tanaka A, Hirota A, Miwa T, Miyabuchi Y (2018) Distribution and mass of tephra-fall deposits from volcanic eruptions of Sakurajima Volcano based on posteruption surveys. Bull Volcanol 80: 42. doi.org/10.1007/s00445-018-1215-3.

Poulidis AP, Takemi T, Iguchi M (2019) Experimental high-resolution forecasting of volcanic ash hazard at Sakurajima, Japan. J Disaster Research 14: 786–797. doi.org/10.20965/jdr.2019.p0786.

Poulidis AP, Takemi T, Iguchi M, Renfrew IA (2017) Orographic effects on the transport and deposition of volcanic ash: A case study of Mount Sakurajima, Japan. J Geophys Res Atmos 122: 9332–9350. doi:10.1002/2017JD026595.

Pyle DM (1989) The thickness, volume and grain size of tephra fall deposits. Bull Volcanol 51: 1–15. doi.org/10.1007/BF01086757.

Rose WI (1993) Comment on 'another look at the calculation of fallout tephra volumes' by Judy Fierstein and Manuel Nathenson. Bull Volcanol 55: 372–374. doi.org/10.1007/BF00301148.

Rose WI, Bonis S, Stoiber RE, Keller M, Bickford T (1973) Studies of volcanic ash from two recent Central American eruptions. Bull volcanol 37: 338-364. doi.org/10.1007/BF02597633.

Sulpizio R (2005) Three empirical methods for the calculation of distal volume of tephra-fall deposit. J Volcanolo Geotherm Res 145: 315–336. doi.org/10.1016/j.jvolgeores.2005.03.001.

Sparks RSJ, Bursik MI, Ablay GJ, Thomas RME, Carey SN (1992) Sedimentation of tephra by volcanic plumes. Part 2: controls on thickness and grain-size variations of tephra fall deposits. Bull volcanol 54: 685-695. doi.org/10.1007/BF00430779.

Suzuki Y, Nagai M, Maeno F, Yasuda A, Hokanishi N, Shimano T, Ichihara M, Kaneko T, Nakada S (2013) Precursory activity and evolution of the 2011 eruption of Shinmoe-dake in Kirishima volcano -insights from ash samples-. Earth Planet Space 65: 591-607. doi.org/10.5047/eps.2013.02.004.

Tajima Y (2014) Eruptive History and Evaluation of Shinmoedake Volcano and Ebinokogen Volcanic Area of Kirishima Volcanoes for the Past 10,000 Years in Kyushu, Japan. Ph.D. thesis of Kagoshima University, p.205. (in Japanese).

Tajima Y, Hayashi S, Yasuda A, Itoh H (2013a) Tephrostratigraphy and eruptive history of Shinmoedake volcano of the Kirishima volcanoes, Kyushu, Japan. The Quaternary Research 52: 151-171 (in Japanese). doi.org/10.4116/jaqua.52.151.

Tajima Y, Tamura K, Yamakoshi T, Tsune A, Tsurumoto S (2013b) Ellipse-approximated isopach maps for estimating ashfall volume at Sakurajima volcano. Bull Volcanol Soc Japan 58: 291-306. doi.org/10.18940/kazan.58.1_291.

Takarada S, Hoshizumi H, Miyagi I, Nishimura Y, Miyabuchi Y, Miura D, Kawanabe Y (2002) Proximal deposits of the Usu 2000 eruption. Bull Geol Surv Japan 47: 645–661 (in Japanese). doi.org/10.18940/kazan.47.5_645.

Takarada S, Oikawa T, Furukawa R, Hoshizumi H, Itoh J, Geshi N, Miyagi I (2016) Estimation of total discharged mass from the phreatic eruption of Ontake Volcano, central Japan, on September 27, 2014. Earth Planets Space 68: 138. doi.org/10.1186/s40623-016-0511-4.

Takarada S et al. (2001) Volcanic ashfalls from the Usu 2000 eruption and situation at the source area. Bull Geol Surv Japan 52: 167–179 (in Japanese). doi.org/10.9795/bullgsj.52.167.

Walker GPL (1980) The Taupo pumice: product of the most powerful known (ultraplinian) eruption? J Volcanol Geotherm Res 8: 69–94. doi.org/10.1016/0377-0273(80)90008-6.

Walker GPL (1981) Plinian eruptions and their products. Bull Volcanol 44: 223–240. doi.org/10.1007/BF02600561.

Figures

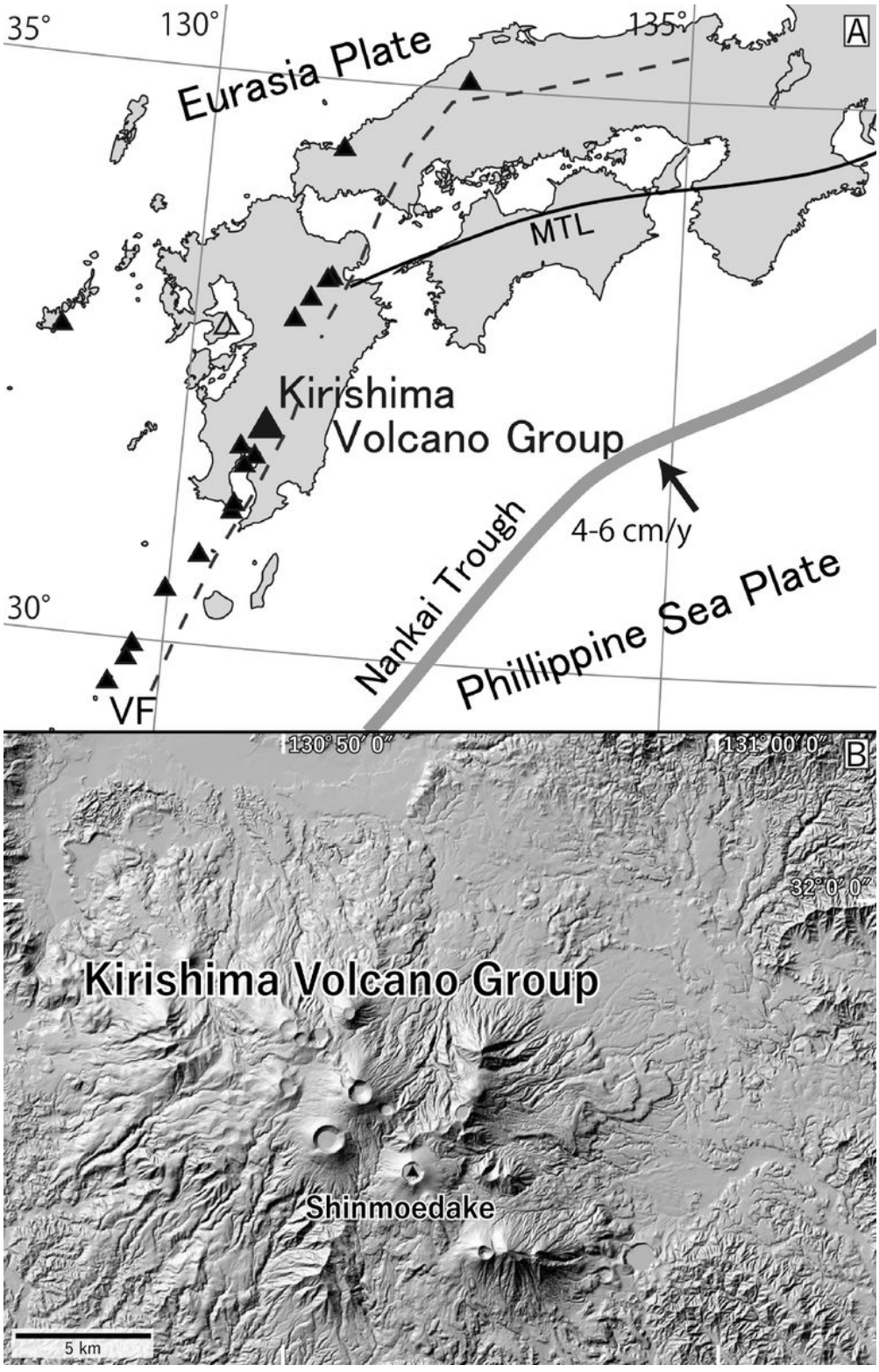

Figure 1

Location index map of the Kirishima Volcano Group. A: Index map of western Japan. B: Shading relief map of Kirishima Volcano Group obtained using the website of the Geospatial Information Authority of Japan (GSI).

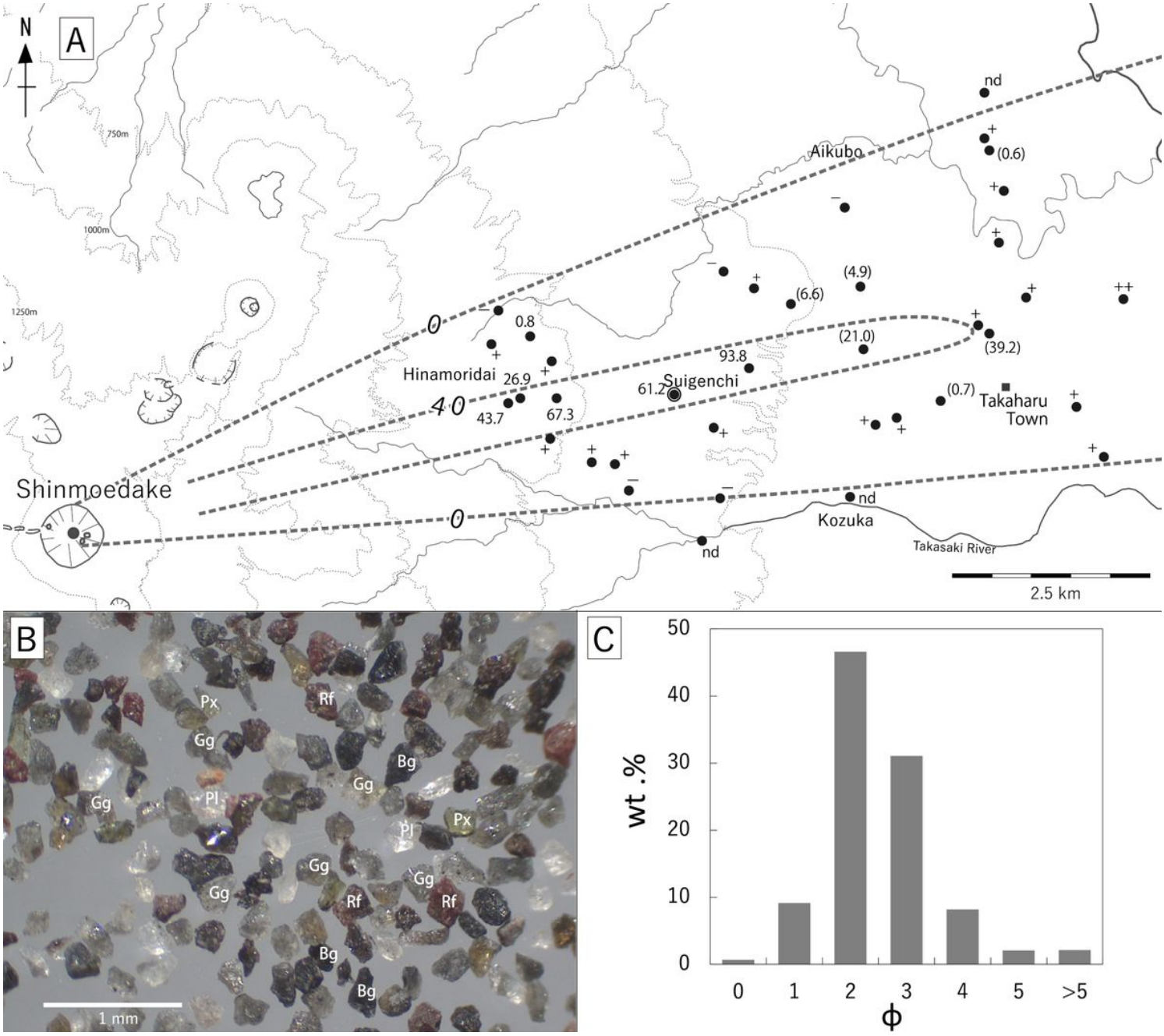

Figure 2

Ashfall of the June 27, 2018 eruption. A: Ashfall distribution map. Numerical values are the amounts of ashfall (g/m2). Values with parentheses have lower accuracy. Gray dashed lines are the 0 and 40-g/m2 isopleths obtained via the field survey. B: The particle component of the deposit at Suigenchi (61.2 g/m2); Bg: Black glass, Gg: Gray glassy fragment, Rf: Red fragment, Pl: Plagioclase, Px: Pyroxenes. C: Grain-size distribution of ashfall at Suigenchi (61.2 g/m2).

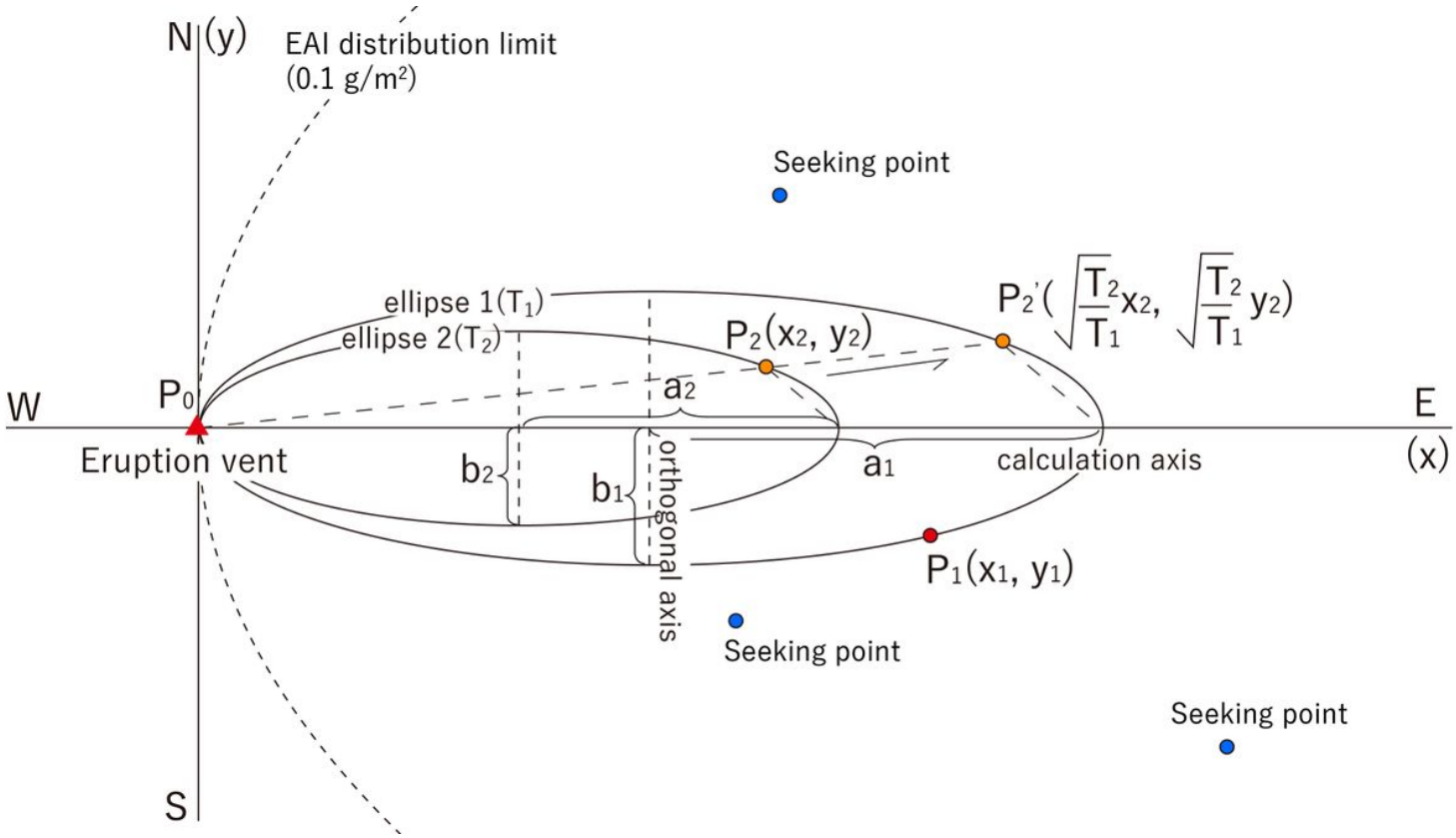

Figure 3

Conceptional model of the ellipse-approximate isopach (EAI) analysis modified from Tajima et al. (2013b). Details are provided in the “EAI analysis method” section.

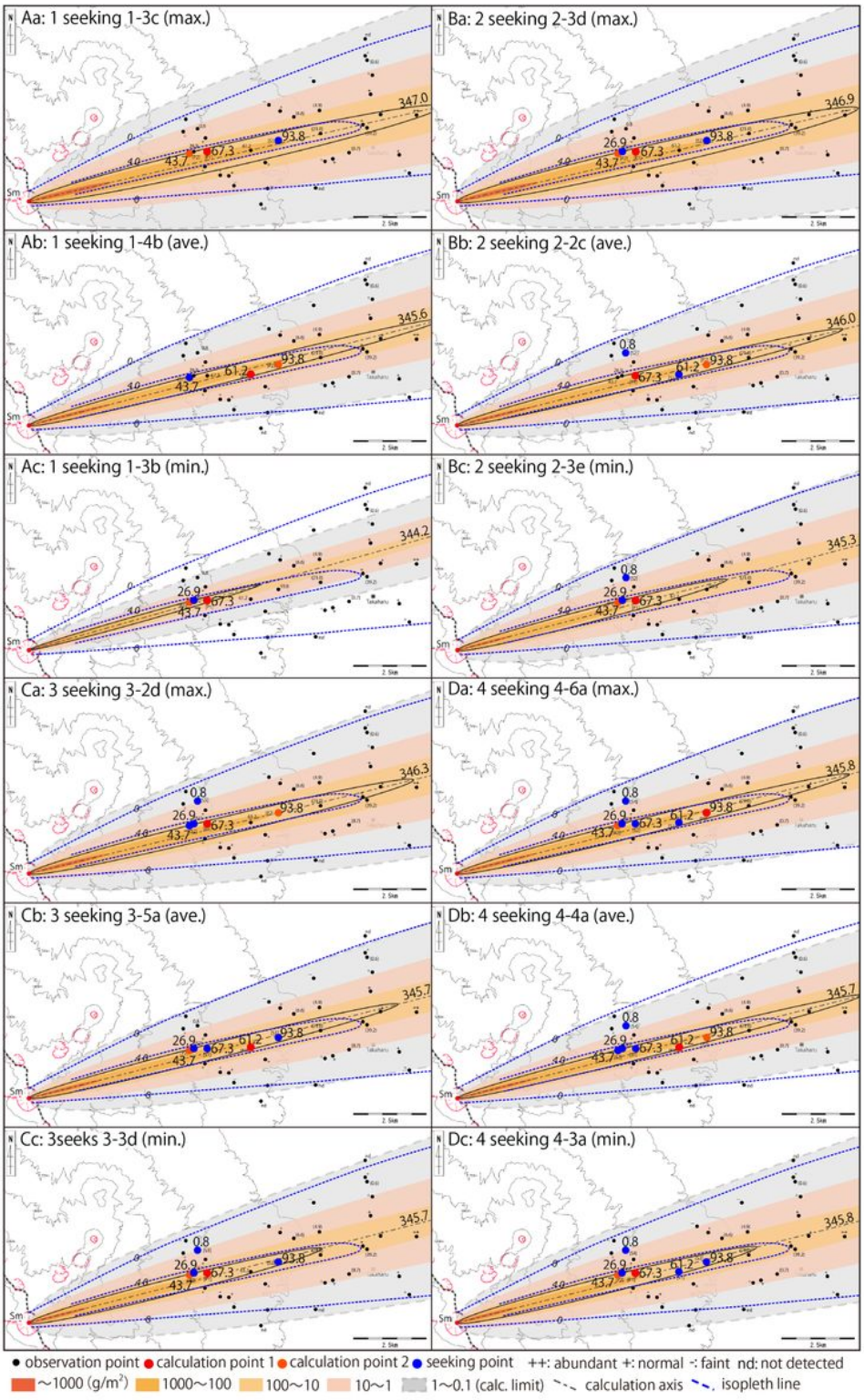

Figure 4

Calculation results of the EAI distributions for the eruption at 15:34 on June 27. Aa–c: Maximum, average, and minimum volumes of the one-point seeking results. Ba–c: Maximum, average, and minimum volumes of the two-point seeking results. Ca–c: Maximum, average, and minimum volumes of the three-point seeking results. Da–c: Maximum, average, and minimum volumes of the four-point seeking results. Numerical values are the amounts of ashfall (g/m2) to the points and axis angle (°) of

the calculation. Blue dashed lines are the 0 and 40-g/m2 isopleths obtained via the field survey, and the black line is the 40-g/m2 isopleth obtained via the EAI calculation.

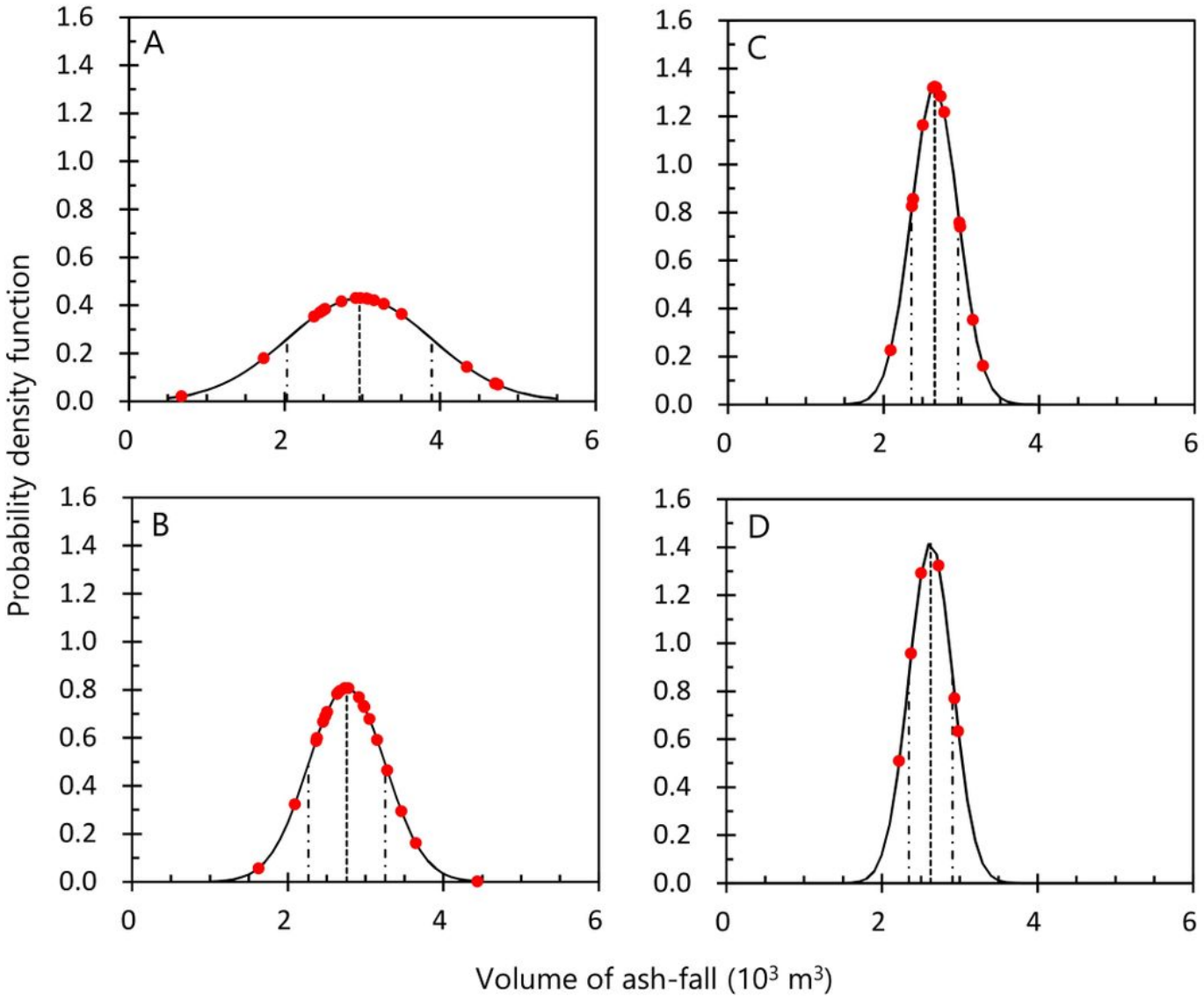

Seeking cases	Axis angle (°)			Aspect ratio			EAI volume ($\times 10^3$ m^3)			
	min.	ave.	max.	min.	ave.	max.	min.	ave.	max.	SD
A: 1-point	344.2	345.9	347.0	0.026	0.042	0.057	0.68	2.96	4.74	0.93
B: 2-point	345.3	345.9	346.9	0.034	0.043	0.056	1.62	2.76	4.44	0.49
C: 3-point	345.6	345.8	346.3	0.035	0.043	0.054	2.09	2.66	3.28	0.30
D: 4-point	345.7	345.9	346.1	0.035	0.043	0.052	2.22	2.63	2.98	0.28

min.: minimum, ave.: average, max.: maximum, SD: Standard deviation

Figure 5

Probability density function of the EAI volume with one to four seeking points. The table at the bottom denotes the EAI analysis results with different point-seeking numbers for the small eruption of Shinmoedake volcano on June 27, 2018.

Supplementary Files

This is a list of supplementary files associated with this preprint. Click to download.

- GraphicalAbs01.jpg
- Shinmoedakeaxissupplementaly.pdf